EFFECT OF PHOSPHOROUS/BORON DOPING PROFILE DIFFERENCES ON THE PERFORMANCE OF SILICON SOLAR CELLS

A. NAWAZ[a], S. TAHIR[a,b,*], A. ALI[a], M. I. ARSHAD[a], K. MAHMOOD[a], S. SIRAJ[a], Y. MUDDASSIR[a]
[a]*Government College University Faisalabad, 38000, Pakistan*
[b]*University of New South Wales, Australia*

This research work was done under title "Effect of phosphorous/boron doping profile differences on the performance of silicon solar cells". Emitter diffusion either phosphorous or boron is quite challenging in photovoltaic industry. It directly affects the emitter saturation current density and the emitter quantum efficiency of silicon solar cells. Our main objective was to make the comparison of both phosphorous and boron diffused emitters for different peak dopant concentrations in silicon solar cells. It was done by using EDNA 2 simulations. We used different parameters in EDNA 2 and simulated the high efficiency solar cells with boron as back ground and phosphorous as emitter. Then we simulated the solar cells with phosphorous as back ground and boron as emitter. We varied the peak dopant concentration of phosphorous as well boron from 1.6E+17 to 3.9E+20. The best internal quantum efficiency of emitter for phosphorous diffused emitters was 95.1 %, obtained at 1.6E19 (cm^{-3}) with an effective emitter depth of 0.675 (µm). However, the best internal quantum efficiency of emitter for boron diffused emitters was 80.6 %, obtained at 3.9E19 (cm^{-3}). It has an effective emitter depth of 0.732 (µm) that is greater than obtained from phosphorous diffused emitters. We concluded that the phosphorous diffused emitters have much better performance than boron diffused emitter in silicon solar cells. They have better internal quantum efficiency of emitters at lower peak dopant concentration. They have lower emitter sheet resistance with lower effective emitter depth, as also required during silicon solar cell fabrication.

(Received November 20, 2019; Accepted February 7, 2020)

Keywords: Silicon solar cell, Phosphorous, Boron, EDNA 2 simulations, Peak dopant concentration (cm^{-3}), Emitter internal quantum efficiency, IQE_e (%).

1. Introduction

A solar cell is an electrical device which is made up of pure silicon and also defined as photovoltaic cell over the decades. Silicon solar cells were demonstrated as first bipolar devices which are involved in conversion of direct sunlight into electrical energy by using the photoelectrical effect (Bagher, Vahid, and Mohsen, 2015; Bube and Bube, 1998; Goetzberger and Hoffmann, 2005). The evolution of silicon solar power has started to give an appreciable contribution of about 4% of the average electricity in the European countries and has more than 7% contributions in other countries like Germany and Italy (Andreani et al., 2019 ; Fraunhofer, 2014; Jager-Waldau, 2017). The generation of electricity from solar energy has increased with high rate maximum 45% per year worldwide (Hosenuzzaman et al., 2015; Kabir et al., 2018).

Silicon solar power is cost effective with an increased efficiency of solar cells by using the semiconductor materials to generate electricity (Jin, 2018). The science behind harnessing the solar energy is photovoltaic. The photovoltaic effect is the production of voltage and electric flow in a material upon introduction to light and is a chemical and physical property material. The photovoltaic and photoelectric effects relate with each other; in either case light is consumed making excitation of electron or other charge transporter a higher vitality state (Green, 2018). The primary differentiation is that the term photoelectric effect is presently typically utilized when electron is shot out of the material for the most part in to a vacuum and photovoltaic effect utilized

* Corresponding author: sofetahir@gmail.com

when the energized charge transporter is as yet contained inside the material. In both the cases an electric potential or voltage is delivered by the division of charges (Luque, and Marti, 1997).

Photovoltaic cells that are made up of silicon, consists of a metallic grid which forms one of the electric contacts and allows the light to fall on the semiconductor diode or p-n junction. Anti-reflective layer, that is silver nitrate is coated in between the metallic grid, it allows the light to be completely absorbed and prevents the light from reflecting and allows the major amount of light to fall on p-n junction (Green, 2000). The other electric contact is the metallic layer which is behind the PV cell. When light falls on the p-n junction electron-hole gaps are generated on p-n junction; the electrons move towards n-type and get segregated and the holes move towards p-type and get segregated. When these two ends are connected to an external circuit we can see movement of electrons, thus obtaining current which is known as PV current. This current is generated until the sunlight is falling on the PV industry.

P-type silicon has a lower surface quality than N-type silicon, so it is layered at the rear of the cell, as most of the light is absorbed at the top of the cell. Therefore, the back of the cell is the positive terminal whereas the front of the cell is the negative terminal. At the front surface, a large amount of light is absorbed. A large amount of the carriers sparked off by the incoming light are generated within the *p-n* junction's diffusion length, by formatting very thin (<1 μm) front layer. In order to conduct the generated electricity without resistive loses, the front junction is doped to a sufficient level. Though, the quality of material is reduced to the extent that carriers recombine before reaching the junction due to extreme levels of doping.

The "quantum efficiency" (Q.E.) is the portion of the quantity of moles of item to the quantity of moles of photons absorbed. The quantum effectiveness attainably is given as energy or as a component of wavelength. The quantum productivity is unity for the situation when all photons of a specific wavelength are retained and the subsequent minority transporters are gathered at that specific wavelength. The quantum productivity is zero for the situation for photons with energy beneath the band gap. Since, the power from the AM1.5 contained in such low wavelengths is low in this manner the quantum proficiency of a silicon solar based cell is commonly not estimated much underneath 350 nm.

The impact of optical losses, for example, transmission and reflection of a silicon solar cell are incorporated in the external quantum efficiency. In any case, it is mostly helpful to observe the quantum efficiency of the light left after the loss of reflected and transmitted light. The productivity with which photons can create collectable carriers without being reflected or transmitted out of the cell is alluded to as internal quantum efficiency.

External Quantum Efficiency (EQE) is the ratio of the number of collected charge carriers by the solar cell to the number of incident photons on the solar cell from outside. Whereas the Internal Quantum Efficiency (IQE) is the ratio of the number of collected charge carriers by the solar cell to the number of incident photons absorbed by the solar cell from outside.

The EQE is always smaller than the IQE. It can be considered that the active layer of the solar cell is not able to make effective use of the photons if IQE is low. IQE can be measures by measuring the EQE of the solar device at first, then measuring its reflection and transmission; and finally combining this data to calculate the IQE.

EDNA 2 figures recombination in a profoundly doped silicon region, for example, an emitter or a rear surface field. It calculates the saturation current density of the J_{0E} emitter and the internal quantum efficiency for a self-assertive doping profile. It may be utilized to calculate the surface recombination rate of an emitter from an experimentally measured J_{0E} (K.R. McIntosh, P.P. Altermatt, 2010).

The EDNA 2 calculation starts by stacking the foundation and dopant profiles of the emitter and ascertaining the resistance of the emitter sheet in balance. The sheet resistance calculator gives a clarification of the functions used to produce the emitter profile and the equations used to ascertain the sheet resistance.

2. Materials and methods

The silicon solar cells were simulated by using phosphorous as well as boron emitter. The study was made for different peak concentrations (N_{max}) of both phosphorous and boron diffused emitters in silicon solar cells.

EDNA 2 simulation tool was used during this research work:

2.1. Silicon solar cells simulated by using Phosphorous diffused emitters

We have used EDNA 2 modelling to study the effect of phosphorous diffused emitters. EDNA 2 can calculate the recombination in a heavily doped region of silicon, such as an emitter or a back-surface field. We determined the emitter saturation current density J_{oe}, Emitter sheet resistance R_{sh} and the internal quantum efficiency (*IQE*) for an arbitrary dopant profile of phosphorus diffused emitters. It was done by using different values of N_{max} (cm^{-3}) of phosphorous diffused emitters as well as Boron diffused emitters.. It can assist their optimisation for practical solar cells as well. We have used different recombination models, material inputs and generation inputs. The simulation with EDNA 2 were done at the temperature of 300 K and the specified voltage ($V_{j,spec}$) of 0.55V. We selected the material inputs for background as well as for emitter of silicon solar cells.

At first, in the background boron was used as a dopant species with concentration N_B of 1E16 cm^{-3} and the bulk resistivity ρ_B of 1.46 ohm-cm. Then we selected phosphorous as dopant species of emitter in the simulation of silicon solar cells. We have used the Gaussian profile for these simulations. In this work, (156 X 156) mm *p*-type silicon wafer was used for the simulations of solar cell.

We have applied the following models: Klaassen's mobility model, Altermatt's dopant ionization model, Richter's Auger recombination model, Passler's Egi model with an Egi multiplier of 1.00547, Schenk's BGN model, Sentaurus's DOS model, and Fermi-Dirac statistics. The list of references for the above given models is in reference (Shanmugam et al., 2016). We have used the SRH parameters for emitter as Et=Ei,τ_{n0} = 100 µs and τ_{p0} = 0.12 µs. By using these models and parameters, we have found the emitter sheet resistance (R_{sh}) and corresponding recombination current densities (J_{0e}) for phosphorous doping profiles with N_{max} (cm^{-3}) varying from 1.6E17 to 3.9E20. We have also determined the emitter depths and internal quantum efficiencies for various phosphorous doping concentrations in silicon solar cell simulations. We took the outputs under no illumination (dark) as well as under illumination (light).

2.2. Silicon solar cells simulated by using Boron diffused emitters

Then in the background, phosphorous was used as a dopant species with concentration N_b of 1E16 cm^{-3} and the bulk resistivity ρ_B of 1.46 Ω-cm. We selected boron as dopant species of emitter in the simulation of silicon solar cells. We have used the Gaussian profile for these simulations.

Again, we have applied the same models: Klaassen's mobility model, Altermatt's dopant ionization model, Richter's Auger recombination model, Passler's Egi model with an Egi multiplier of 1.00547, Schenk's BGN model, Sentaurus's DOS model, and Fermi-Dirac statistics. The list of references for the above given models is in reference (Shanmugam et al., 2015). We have used the SRH parameters for emitter as Et=Ei,τ_{n0} = 100 µs and τ_{p0} = 0.12 µs. By using these models and parameters, we have found the emitter sheet resistance (R_{sh}) and corresponding recombination current densities (J_{oe}) for boron doping profiles with N_{max} (cm^{-3}) varying from 1.6E17 to 3.9E20. We have also determined the emitter depths and internal quantum efficiencies for various boron doping concentrations in silicon solar cell simulations. We took the outputs under no illumination (dark) as well as under illumination (light).

3. Results and discussion

3.1. Silicon solar cells simulated by using Phosphorous/Boron diffused emitters

EDNA 2 was used to simulate silicon solar cells for different doping profiles of both phosphorous and boron diffused emitters at room temperature (300 K). EDNA 2 modelling parameters are shown in Table 1.

Table 1. EDNA 2 modelling parameters.

N_{max}	Emitter SRH			Surface SRH			Simulated outputs		
cm^{-3}	E_t	τ_{n0} µs	τ_{p0} µs	Q_f/q	E_t	S_{p0}	R_{sh} (ohm/sq)	J_{0e} (fA/cm^2)	IQE (%) at 350 nm
For P 1.6E19	$E_t=E_i$	100	0.12	$2.8x10^{12}$	$E_t=E_i$	$2.0x10^4$	130	78.9	95.1
For B 3.9E19	$E_t=E_i$	100	0.12	$2.8x10^{12}$	$E_t=E_i$	$1.0x10^4$	102	216	80.6

By using the parameters given in Table 1, we simulated silicon solar cells with phosphorous as well as boron diffused emitters. We have selected the monochromatic light as a spectrum of the generation inputs. Absorption coefficient α of 1.77E6 (cm^{-1}) was always constant. For incident light J_{inc} was 40 (mA/cm^2) where the transmission fraction was 1. Our main objective was to change the peak dopant concentration N_{max} (cm^{-3}) for phosphorous diffused emitters in silicon solar cell simulations. Our simulations were based to find the following major outputs:

1. Emitter sheet resistance at equilibrium ρ_{sq} (Ω/sq)
2. Emitter saturation current at 0.55V J_{oe} (fA/cm^2)
3. Emitter collection efficiency at short-circuit IQE_e (%)

We have found these outputs by varying the peak dopant concentration N_{max} (cm^{-3}) from 1.6E+17 to 3.9E+20 for both phosphorous and boron diffused emitters in silicon solar cells simulations. The results showed different depths of emitters for different dopant concentrations of phosphorous and boron.

3.2. Silicon solar cells simulated by using phosphorous diffused emitter with N_{max} (cm^{-3}) varying from 1.6E17 to 3.9E20

The Table 2 showed the different dopant concentrations of phosphorous diffused emitters and the corresponding depths of emitters. It also showed our required outputs of emitter sheet resistance ρ_{sq} (Ω/sq), emitter saturation current J_{oe}(fA/cm^2) and the emitter collection efficiency IQE_e(%). It showed that the emitter doping concentration was varied from 1.6E+17 (cm^{-3}) to 3.9E+20 (cm^{-3}) with an increase of emitter depth 0.182 to 0.867 (µm). The corresponding emitter sheet resistance was decreased from the 4190 to 11.2 (Ω/sq). The emitter saturation current density was increased from 52.4 (fA/cm^2) to 124 (fA/cm^2). The emitter collection efficiency was decreased from 100 % to 19.6 %. To study the effect of peak dopant concentration of phosphorous in an emitter of silicon solar cells, we have drawn a graph between N_{peak} (cm^{-3}) and emitter depth (µm). The results are shown in Fig. 1.

Table 2. Phosphorous diffused emitter with N_{max} (cm^{-3}) varying from 1.6E17 to 3.9E20.

Emitter dopant concentration N_{peak}(cm^{-3})	Emitter sheet resistance ρ_{sq} (Ω/sq)	Emitter saturation current J_{oe} (fA/cm^2)	Emitter collection efficiency IQE_e(%)	Effective emitter depth (μm)
1.6E+17	4190	52.5	100%	0.182
2.0E+17	2990	57.8	99.9%	0.231
2.5E+17	2310	61.2	99.9%	0.272
3.0E+17	1930	63.2	99.9%	0.302
3.5E+17	1700	63.5	99.9%	0.32
3.9E+17	1550	64.5	99.8%	0.336
1.6E+18	610	99.0	99.4%	0.491
2.0E+18	533	70.7	99.2%	0.516
2.5E+18	469	69.5	99.1%	0.527
3.0E+18	419	71.8	98.9%	0.55
3.5E+18	381	71.3	98.7%	0.557
3.9E+18	355	74.3	98.5%	0.577
1.6E+19	130	78.9	95.1%	0.675
2.0E+19	109	79.3	94.3%	0.685
2.5E+19	91.3	84.3	93.2%	0.712
3.0E+19	78.8	85.7	92.2%	0.72
3.5E+19	69.5	87.6	91.2%	0.727
3.9E+19	63.6	89.3	90.4%	0.732
1.6E+20	19.9	135	59.5%	0.811
2.0E+20	16.8	137	50.0%	0.82
2.5E+20	14.4	140	39.7%	0.849
3.0E+20	12.9	136	31.2%	0.856
3.3Es+20	12.2	133	26.8%	0.86
3.5E+20	11.8	132	24.2%	0.862
3.9E+20	11.2	124	19.6%	0.867

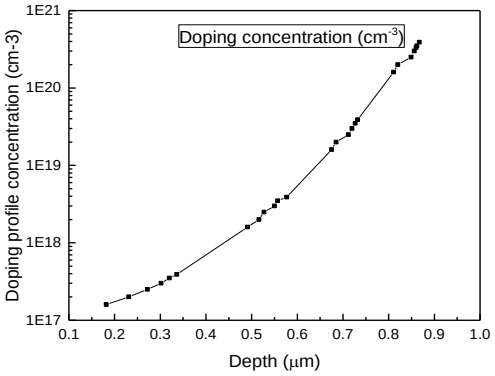

Fig. 1. The effect of 1.6E17 to 3.9E20 (cm^{-3}) N_{max} of phosphorous on emitter depth.

This result showed the relationship between doping profile concentration (cm^{-3}) and the effective emitter depth (μm). Figure 1 showed that the depth of phosphorous diffused emitter is increased with the increase of peak dopant concentration of phosphorous. When the phosphorous concentration was increased from 1.6E+17 to 3.9E+20 (cm^{-3}), then emitter depth was also increased from 0.182 to 0.867μm.

3.3. Silicon solar cells simulated by using boron diffused emitter with N_{max}(cm^{-3}) varying from 1.6E17 to 3.9E20

The Table 3 showed the different dopant concentrations of boron diffused emitters and the corresponding depths of emitters. It also showed our required outputs of emitter sheet resistance

ρ_{sq} (Ω/sq), emitter saturation current J_{oe}(fA/cm^2) and the emitter collection efficiency IQE_e(%).It showed that the emitter doping concentration were varied from 1.6E+17 (cm^{-3}) to 3.9E+20 (cm^{-3}) with an increase of emitter depth 0.172 to 0.867 (µm). The corresponding emitter sheet resistance was decreased from the 9840 to 14.1 (Ω/sq). The emitter saturation current density was increased from 24.5 (fA/cm^2) to 113 (fA/cm^2). The emitter collection efficiency was decreased from 100 % to 53.3%. In order to study the effect of peak dopant concentration of boron in an emitter of silicon solar cells, we have drawn a graph between N_{peak} (cm^{-3}) and emitter depth (µm). The results are shown in Fig. 2.

Table 3. Boron diffused emitter with N_{max}(cm^{-3}) varying from 1.6E17 to 3.9E20.

Emitter dopant concentration N_{peak}(cm^{-3})	Emitter sheet resistance ρ_{sq} (Ω/sq)	Emitter saturation current J_{oe} (fA/cm^2)	Emitter collection efficiency IQE_e(%)	Effective emitter depth (µm)
1.6E+17	9840	24.5	100%	0.172
2.0E+17	6850	26.5	100%	0.22
2.5E+17	5170	29.0	100%	0.261
2.8E+17	4410	30.5	100%	0.288
3.0E+17	4250	31.4	100%	0.291
3.3E+17	3860	32.9	99.9%	0.306
3.5E+17	3620	33.8	99.9%	0.32
3.9E+17	3270	35.8	99.9%	0.336
1.6E+18	1160	204	98.6%	0.491
2.0E+18	1000	545	96.2%	0.516
2.5E+18	873	4100	78.4%	0.527
2.8E+18	808	7910	27.1%	0.547
3.0E+18	773	7470	1.54%	0.55
3.3E+18	727	6890	1.55%	0.555
3.5E+18	700	6550	1.58%	0.557
3.9E+18	652	5970	1.73%	0.562
1.6E+19	219	786	60%	0.675
2.0E+19	181	542	67.9%	0.685
2.5E+19	150	386	73.6%	0.695
2.8E+19	136	329	75.8%	0.717
3.0E+19	128	300	77%	0.72
3.3E+19	118	265	78.5%	0.724
3.5E+19	112	246	79.3%	0.727
3.9E+19	102	216	80.6%	0.732
1.6E+20	29.5	109	78.9%	0.811
2.0E+20	24.3	112	74.7%	0.82
2.3E+20	22.0	113	72.7%	0.831
2.5E+20	20.1	115	69.0%	0.849
2.8E+20	18.3	116	65.5%	0.853
3.0E+20	17.3	116	63.2%	0.856
3.3E+20	16.0	15	59.8%	0.86
3.5E+20	15.3	115	57.6%	0.862
3.9E+20	14.1	113	53.3%	0.867

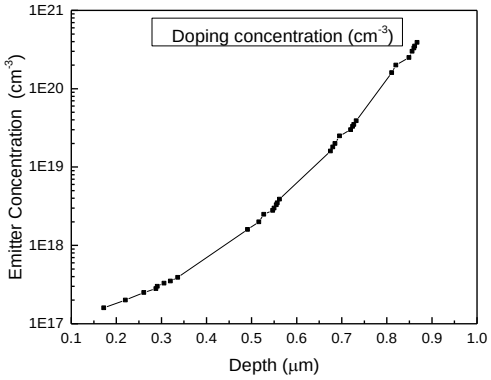

Fig. 2. The effect of 1.6E17 to 3.9E20 (cm^{-3}) N_{max} of boron on emitter depth.

This general result showed the relationship between doping profile concentration (cm^{-3}) and the effective emitter depth (μm). Figure 2 showed that the depth of boron diffused emitter is increased with the increase of peak dopant concentration of boron. When the boron concentration was increased from 1.6E+17 to 3.9E+20(cm^{-3}), then emitter depth was also increased from 0.172 to 0.867 μm.

3.4. Doping profile differences due to various N_{max}(cm^{-3}) of Phosphorous/Boron in emitters

We have simulated both phosphorous and boron diffused emitters in EDNA 2 for various peak dopant concentrations. The results obtained for doping profiles of phosphorous diffused emitters for N_{max} (cm^{-3}) varying from 1.6E17 to 3.9E20 (cm^{-3}) showed that their performance are much better for the peak dopant concentration ranging from 1.6E19 to 3.9E19 (cm^{-3}). For this range of peak phosphorous concentration in emitters, the emitter sheet resistance was decreased from 130 to 63.6 (Ω/sq). The emitter saturation current density was increased from 78.9 to 89.3 (fA/cm^2). It gave us a good relationship between emitter sheet resistance and the emitter saturation current density. However the best internal quantum efficiency of emitter for phosphorous diffused emitters was 95.1 %, obtained at 1.6E19 (cm^{-3}). It has an effective emitter depth of 0.675 (μm).

However, the results obtained for doping profiles of boron diffused emitters for N_{max} (cm^{-3}) varying from 1.6E17 to 3.9E20 (cm^{-3}) showed that their performance are good for the peak dopant concentration ranging from 2.5E19 to 3.9E19 (cm^{-3}). For this range of peak boron concentration in emitters, the emitter sheet resistance was decreased from very high value of 150 (Ω/sq) to 102 (Ω/sq). This is quiet higher than that obtained from phosphorous diffused emitters in silicon solar cells. The emitter saturation current density was changed from 386 to 216 (fA/cm^2). However the best internal quantum efficiency of emitter for boron diffused emitters was 80.6 %, obtained at 3.9E19 (cm^{-3}). It has an effective emitter depth of 0.732 (μm) that is greater than obtained from phosphorous diffused emitters.

4. Conclusions

In this research work we concluded that the phosphorous diffused emitters in silicon solar cells have much better performance than boron diffused emitter in silicon solar cells. They have better internal quantum efficiency of emitters at lower peak dopant concentration. They have lower emitter sheet resistance with lower effective emitter depth, as also required during silicon solar cell fabrication.

References

[1] L. C. Andreani, A. Bozzola, P. Kowalczewski, M. Liscidini, L. Redorici, Advances in Physics: X **4**(1), 1548305 (2019)

[2] A. M. Bagher, M. M. A. Vahid, M. Mohsen, American Journal of optics and Photonics **3**(5), 94 (2015).

[3] R. H. Bube, Photovoltaic materials, 1998.

[4] I. Fraunhofer, 2014, Photovoltaics report. Disponible sur: http://www. ise. fraunhofer. de/en/downloads-englisch/pdf-files-englisch/photovoltaics-report-slides. pdf/view, rapport publié en.

[5] A. Goetzberger, Photovoltaic solar energy generation **112**, 2005.

[6] A. Goetzberger, J. Knobloch, B. Voss, 1998, Crystalline silicon solar cells. editorial John Wiley & Sons Ltd, 1.

[7] M. A. Green, Mater. Sci. Eng. B, 2000.

[8] M. A. Green, High-efficiency silicon solar cell concepts McEvoy's Handbook of Photovoltaics, pp. 95, 2018, Elsevier.

[9] M. R. Hoffmann, S. T. Martin, W. Choi, D. W. Bahnemann, Chemical reviews **95**(1), 69 (1995).

[10] M. Hosenuzzaman, N. A. Rahim, J. Selvaraj, M. Hasanuzzaman, A. A. Malek, A. Nahar, Renewable and Sustainable Energy Reviews **41**, 284 (2015).

[11] A. Jäger-Waldau, Sustainability **9**(5), 783 (2017).

[12] E. Kabir, P. Kumar, S. Kumar, A. A. Adelodun, K.-H. Kim, Renewable and Sustainable Energy Reviews **82**, 894 (2018).

[13] A. Luque, A. Martí, Physical review letters **78**(26), 5014 (1997).

[14] K. R. McIntosh, P. P. Altermatt, 2010, June, A freeware 1D emitter model for silicon solar cells. In 2010 35th IEEE Photovoltaic Specialists Conference (pp. 002188-002193). IEEE.

[15] V. Shanmugam, A. Khanna, P. K. Basu, A. G. Aberle, T. Mueller, J. Wong, Solar energy materials and solar cells **147**, 171 (2016).